Transmission, reflection and energy exchanges for waves in finite one-dimensional PT-symmetric periodic structures

Darryl McMahon

Centre for Marine Science and Technology, Curtin University, Perth, Australia

ABSTRACT

Time reversibility of waves within a periodic structure constrains their properties but allows both elastic and inelastic scattering. Time reversible elastic scattering leads to Bloch-Floquet waves (BFW) exhibiting passing and stopping bands for an infinite periodic structure, and time reversible inelastic scatterers likewise exhibits passing and stopping bands but only for a particular domain of parameters. Physical realizations of time reversible inelastic scatterers have exploited parity-time (PT) symmetry with two parts, each of which is time irreversible while mirrored such that their PT combination is symmetric. The second propagation domain for inelastic scattering (called "broken" PT-symmetry) is entirely a passing band that transmits and reflects more wave energy than in the input wave. In the "broken" domain for m=2n scatterers, where n is any odd integer, amplification peaks at the same discrete wavenumbers as well-known Bragg reflections. A property of PT-symmetric scatterers at the boundary of its two domains is unidirectional "invisibility" where there are no reflections for one of the two possible incident wave directions. A PT-symmetric periodic structure is shown here to also have bidirectional "invisibility" at certain discrete wavenumbers.

1 INTRODUCTION

The problem of wave propagation in a periodic structure is long standing (Brillouin 1953) and solved most simply for an infinite structure without boundary effects. More general solutions for any length periodic structure are determined from the eigenvalues and eigenvectors for scattering by just one cell within the structure (McMahon 2018a,b). The most general possible 2x2 complex scattering matrix $\mathbf{S}$ consists of 8 independent parameters. In this form wave propagation for periodic structure waves (PSW) allows deviations from common simplifying properties. One such property is reciprocity for a linear medium meaning both the amplitude and phase at a reception point are unchanged by swapping the source and receiver positions (Pierce,1981). For reflections by a scatterer in a 1D system, reciprocity is assured since the source and receiver points are on the same side so that interchanging their positions makes no difference to the wave amplitude and phase irrespective of scatterer properties. For forward transmission however, reciprocity nontrivially constrains the scatterer phase shifts to be the same for both incident wave directions.

In recent years there has been a growing realization that nonreciprocal wave propagation has some practical advantages (Fleury et al 2015). A potential application is increased attenuation of waves propagating along a periodic structure (McMahon 2017b). It is highly desirable that such an application of nonreciprocity only need wave-scatterer dissipative energy losses. However satisfying both nonreciprocity and passive system energy losses only gives incoherent wave solutions (McMahon 2017a, 2018a), equivalent to waves whose phases are randomized by scatterers. This is a significant limitation since scatterers with thicknesses much smaller than a wavelength are unlikely to randomize wave phases. Nonreciprocal scattering of coherent waves in a periodic structure entails phase sensitive inelastic scattering (McMahon 2018b) and carries the implication that nonreciprocal scatterers are active systems. This is manifested in a practical realization of a 1D nonreciprocal acoustic scatterer which consists of a nonlinear material sandwiched on one side by an amplification layer and the other side by an attenuation layer, hence is an active system (Gu et al 2016).

Another relatively recent development in wave theory and experimentation are PT-symmetric systems (see review El-Ganainy et al 2018). The concept was originally inspired by the discovery of physically realizable non-Hermitian Hamiltonians in quantum mechanics, with real energy levels in one domain and complex energy levels in a second domain called broken PT-symmetry (Bender 2007, El-Ganainy et al 2018). Experimental realizations of PT-symmetric acoustic systems are internally asymmetric with two parts, each of which is time irreversi-

ble while mirrored such that their PT combination is symmetric. (Shi et al 2016, Auregan and Pagneux 2017). The theory and properties of PT-symmetric 1D periodic structures are topics of this paper.

Section 2 derives for a single scatterer the 1D scattering matrix $\mathbf{S}$ constrained to satisfy time-reversal symmetry for both elastic and inelastic scattering. Inelastic scattering reproduces known results for PT-symmetry when forward scattering reciprocity is added, and differs from elastic scattering by allowing two scattering domains. Related theoretical work has been published by Ge et al (2012) and Schomerus (2013). The transfer matrix $\mathbf{M}$, reflection matrix $\mathbf{N}$ and wave-scatterer energy exchanges are derived for waves impinging on a "bare" PT-symmetric scatterer. Subsection 2.1 extends PT scatterer theory to single cells defining matrices $\ddot{\mathbf{M}}$ and $\ddot{\mathbf{N}}$. Formulae for the eigenvalues and eigenvectors of $\ddot{\mathbf{M}}$ and $\ddot{\mathbf{N}}$ written in a form that clearly expose the cell scattering conditions for passing and stopping bands (terminology used here for finite periodic structures although actually stopping waves requires an infinite periodic structure), a wave feature that PT-symmetry has in common with elastic scattering giving rise to BFW. Subsection 2.2 discusses how the scattering properties of finite periodic structures are derived from the eigenvalues and eigenvectors of a single cell, and discusses analytical features of m=2 PT-symmetric scatterers.

Section 3 demonstrates various features of wave propagation in a PT-symmetric periodic structure. This paper shows that the two domains are distinguished by amplified or damped scattering in the PT-symmetric domain and always amplifying in the broken PT-symmetric domain. Further the PT symmetry domain exhibits passing and stopping bands in a periodic structure, whereas the broken domain is entirely a passing band. PT-symmetric scattering makes the difference of average reflection and forward transmitted phase shifts $\delta = \bar{\chi} - \bar{\phi}$ an odd multiple of $\pm\pi/2$, hence causing passing & stopping bands (McMahon 2015, 2016a). For the broken domain δ are even multiples of $\pm\pi/2$. Any deviations of δ from integer multiples of $\pm\pi/2$ make scattering inelastic and generally nonreciprocal (McMahon 2018b). At the boundary of the two domains one of the two possible incident wave directions has zero reflectivity (unidirectional invisibility). A new feature of PT-symmetric periodic structures shown in this paper is bidirectional invisibility at certain discrete wavenumbers. Also shown, for a particular value of forward scattering gain, are wavenumbers in the broken PT-symmetric domain with very high gain (infinite in the absence of dissipation), essentially periodic structure resonances at the same wavelengths as Bragg reflections. This effect only exists for an even number m=2n of scatterers where n is an odd integer.

2 THEORY OF WAVES IN A FINITE PT-SYMMETRIC PERIODIC STRUCTURE

This section specializes the general scattering theory (McMahon 2018b) to PT-symmetric systems. Consider wave scattering by the "bare" scatterer in the n^{th} cell of a 1D periodic stucture. The thickness of a scatterer is b and the distance of the back surface of the n^{th} scatterer from the front surface of the n+1$^{\text{th}}$ scatterer is d. Hence a cell length is d+b. The complex 2x2 transfer matrix $\mathbf{M}$ transforms any complex wave vector $\begin{pmatrix} A_n & B_n \end{pmatrix}^T$ on one side to $\begin{pmatrix} A_{n+1} & B_{n+1} \end{pmatrix}^T = \mathbf{M}\begin{pmatrix} A_n & B_n \end{pmatrix}^T$ on the other side of the n^{th} scatterer (where superscript T denotes matrix transpose). The "A" component is the complex amplitude of a plane wave travelling in the +x direction from a source at $x \to -\infty$ while the "B" component travels in the –x direction from a source at $x \to \infty$. The 8 parameters of $\mathbf{M}$ are easiest understood in terms of 4 complex scattering coefficients $T^{(\pm)}$ and $R^{(\pm)}$ where $T^{(+)}$ and $R^{(+)}$ are forward transmission and reflection coefficients of the "A" component, and $T^{(-)}$ and $R^{(-)}$ apply to the "B" component. From $\mathbf{M}$ written in terms of $T^{(\pm)}$ and $R^{(\pm)}$ the reflection matrix $\mathbf{N}$ can be defined by simply interchanging forward and backward scattering coefficients in $\mathbf{M}$. Further, the scattering matrix $\mathbf{S}$ has the property of transforming waves heading towards a scatterer into waves heading away i.e. $\begin{pmatrix} A_{n+1} & B_n \end{pmatrix}^T = \mathbf{S}\begin{pmatrix} A_n & B_{n+1} \end{pmatrix}^T$. $\mathbf{S}$ has the form

$$\mathbf{S} = \begin{pmatrix} T^{(+)} & R^{(-)} \\ R^{(+)} & T^{(-)} \end{pmatrix} \tag{1}$$

Time reversal symmetry is the condition $\mathbf{S}^{-1}$=$\mathbf{S}^*$ which can be satisfied for both elastic (Maznev et al 2013) and inelastic scattering. Time reversible inelastic scattering can exist externally even though processes within a scatterer may be time irreversible, such as two internal nonlinear parts with mirrored geometry. This makes energy transfers reversible between scatterers and waves (e.g. waves are not phase randomized).

We define phase shifts $\phi^{(\pm)}$ and $\chi^{(\pm)}$ by $T^{(\pm)}=e^{i\phi^{(\pm)}}\left|T^{(\pm)}\right|$ and $R^{(\pm)}=e^{i\chi^{(\pm)}}\left|R^{(\pm)}\right|$, $\bar{\phi}=\left(\phi^{(+)}+\phi^{(-)}\right)/2$, $\bar{\chi}=\left(\chi^{(+)}+\chi^{(-)}\right)/2$. From $\mathbf{S}^{-1}=\mathbf{S}^{*}$ we find $\left|T^{(+)}\right|^2=\left|T^{(-)}\right|^2=|T|^2$ and $R^{(+)}R^{(-)*}=R^{(+)*}R^{(-)}$. Forward scatter phase shifts are unconstrained while the reflection phase shifts satisfy $\sin(\chi^{(+)}-\chi^{(-)})=0$. Two reflection phase shift types can exist, $\chi^{(+)}=\chi^{(-)}$ and $\chi^{(+)}=\chi^{(-)}+(\pm)'\pi$ which can be rewritten as $\chi^{(\pm)}=\bar{\chi}$ and $\chi^{(\pm)}=\bar{\chi}+(\pm)(\pm)'\pi/2$ where two independent sign ambiguities are indicated. Then $\mathbf{SS}^{*}=\mathbf{1}$ has two possible solutions such that

$$|T|^2-e^{2i\delta}\left|R^{(+)}\right|\left|R^{(-)}\right|=1 \tag{2a}$$

$$|T|^2-e^{2i\delta}\left|R^{(+)}\right|\left|R^{(-)}\right|=-e^{2i\left(\chi^{(\pm)}-\bar{\phi}\right)} \tag{2b}$$

A time reversible scatterer must satisfy both Eq.(2a) or (2b). The domain $\chi^{(\pm)}=\bar{\chi}$ applies when $e^{2i\delta}=-1$ (i.e. $\delta=\pm\pi/2,\pm3\pi/2$) and the domain $\chi^{(\pm)}=\bar{\chi}+(\pm)(\pm)'\pi/2$ applies when $e^{2i\delta}=1$ (i.e. $\delta=0,\pm\pi$). Deviations from these two domains of δ imply inelastic nonreciprocal scattering (McMahon 2018b).

An energy flux includes an impedance factor but for convenience we assume units where it can be set to one. The net energy flux incident onto the n^{th} scatterer is $|A_n|^2+|B_{n+1}|^2=\begin{pmatrix}A_n^{*} & B_{n+1}^{*}\end{pmatrix}\begin{pmatrix}A_n & B_{n+1}\end{pmatrix}^T$ and the net output energy flux is $\begin{pmatrix}A_{n+1}^{*} & B_n^{*}\end{pmatrix}\begin{pmatrix}A_{n+1} & B_n\end{pmatrix}^T$. The difference of the input and output fluxes is the wave-scatterer energy exchange $F_{ex}=\begin{pmatrix}A_n^{*} & B_{n+1}^{*}\end{pmatrix}\left(\mathbf{1}-\mathbf{S}^{*T}\mathbf{S}\right)\begin{pmatrix}A_n & B_{n+1}\end{pmatrix}^T$. For elastic scattering $F_{ex}=0$ giving $\mathbf{S}^{-1}=\mathbf{S}^{*T}$ which is the special case of time-reversibility where $\mathbf{S}^{*T}=\mathbf{S}^{*}$ (i.e. $\mathbf{S}$ symmetric). Hence time reversible elastic scattering requires $\chi^{(+)}=\chi^{(-)}\equiv\bar{\chi}$ but allows $\phi^{(+)}\neq\phi^{(-)}$ which is nonreciprocity. From $\det\left(\mathbf{S}^{*}\right)\det\left(\mathbf{S}\right)=1$ for elastic scattering, $\left|T^{(-)}\right|^2=\left|T^{(+)}\right|^2$, $\left|R^{(+)}\right|^2=\left|R^{(-)}\right|^2$ and $\left|T^{(\pm)}\right|^2+\left|R^{(\pm)}\right|^2=1$. These are equivalent to $\left|T^{(\pm)}\right|^2=|T_0|^2$, $\left|R^{(\pm)}\right|^2=|R_0|^2$ and $|T_0|^2+|R_0|^2=1$. From $\mathbf{S}^{-1}=\mathbf{S}^{*T}$ we find $\det\left(\mathbf{S}\right)=T^{(+)}/T^{(-)*}=e^{2i\bar{\phi}}$ and $\det\left(\mathbf{S}\right)=-R^{(+)}/R^{(-)*}=-e^{2i\bar{\chi}}$ which are both satisfied for the case $e^{2i\delta}=-1$. Consequently elastic scattering constrains phase shifts to $\delta=\pm\pi/2,\pm3\pi/2$ which is the single domain giving rise to BFW in a periodic structure. Reciprocity of forward scattering is the same thing as a separate condition P (parity) or mirror symmetry on opposite sides of a scatterer. Then PT-symmetric elastic scattering only needs 2 independent parameters such as $|T_0|$ & $\bar{\phi}$ from which $|R_0|$ & $\bar{\chi}$ can be derived.

Assume that inelastic scattering allows both of the two domains, one with $e^{2i\delta}=-1$ giving rise to passing and stopping bands, and the other with $e^{2i\delta}=1$ which is a passing band. Similar to McMahon 2018b, introduce wave-scatterer energy exchange factors σ_0 and $\sigma_0^{(\pm)}$ where $T^{(\pm)}=e^{i\phi^{(\pm)}}\sigma_0|T_0|$ and $R^{(\pm)}=e^{i\chi^{(\pm)}}\sigma_0^{(\pm)}|R_0|$ where $|T_0|^2+|R_0|^2=1$. Equations (2a,b) allow the two domains

$$\sigma_0{}^2|T_0|^2+\tilde{\sigma}_0{}^2|R_0|^2=1,\ \sigma_0|T_0|\le1,\ \delta=\pm\pi/2,\pm3\pi/2 \tag{3a}$$

$$\sigma_0{}^2|T_0|^2-\tilde{\sigma}_0{}^2|R_0|^2=1,\ \sigma_0|T_0|>1,\ \delta=0,\pm\pi \tag{3b}$$

where $\tilde{\sigma}_0{}^2=\sigma_0^{(+)}\sigma_0^{(-)}$. Elastic scattering is the case $\sigma_0=\sigma_0^{(+)}=\sigma_0^{(-)}=1$ satisfying $\sigma_0|T_0|\le1$ only. Domain $\sigma_0|T_0|>1$ only exists for inelastic scattering. Close to the boundary of the two domains where $\sigma_0|T_0|\to1$ it is possible for $\tilde{\sigma}_0{}^2\to0$ by either $\sigma_0^{(+)}\to0$ or $\sigma_0^{(-)}\to0$. Zero reflection for only one of the incident wave directions has been termed variously “unidirectional invisibility”, “unidirectional tranparency”, “unidirectional reflectivity”

and "unidirectional cloaking" (Lin et al 2011, Longhi 2011, Regensburger et al 2012, Feng et al 2013, Mostafazadeh 2013, Sounas et al 2015, Shi et al 2016,). The condition $\sigma_0|T_0|=1$, $\tilde{\sigma}_0^{\,2}=0$ is an exceptional point (EP) (Shi et al 2016, El-Ganainy et al 2018), a term used in quantum mechanics where Hamiltonians go from Hermitian to non-Hermitian. The transition from $\sigma_0|T_0|<1$ to $\sigma_0|T_0|>1$ has been called a exact PT to broken PT phase transition (phase as analogous to a state of matter), but also named domains in this paper. Eqs.(2a,b) and (3a,b) are only T-symmetric since reciprocity $\phi^{(+)}=\phi^{(-)}$ is not needed to derive them. PT-symmetry in Ge et al 2012 and Schomerus 2013) are equivalent to the reciprocity $\phi^{(+)}=\phi^{(-)}$ together with Eqs.(2a,b,3a,b).

Transfer matrix $\mathbf{M}$ relates the vector $\begin{pmatrix}A_n & B_n\end{pmatrix}^T$ on one side of the n^{th} scatterer to the vector $\begin{pmatrix}A_{n+1} & B_{n+1}\end{pmatrix}^T$ on the other side by $\begin{pmatrix}A_{n+1} & B_{n+1}\end{pmatrix}^T=\mathbf{M}\begin{pmatrix}A_n & B_n\end{pmatrix}^T$. $\mathbf{S}$ given by Eq.(1) can be used to construct $\mathbf{M}$. The reflection matrix $\mathbf{N}$ can be thought of as the transfer matrix for a vector $\begin{pmatrix}X_n & Y_n\end{pmatrix}^T$ but $\mathbf{N}$ is constructed from $\mathbf{M}$ by transformation $T^{(-)}\rightleftarrows R^{(-)}$ and $T^{(+)}\rightleftarrows R^{(+)}$. Then (McMahon 2018b)

$$\mathbf{M}=\frac{1}{T^{(-)}}\begin{pmatrix}T^{(-)}T^{(+)}-R^{(-)}R^{(+)} & R^{(-)}\\ -R^{(+)} & 1\end{pmatrix},\quad \mathbf{N}=\frac{1}{R^{(-)}}\begin{pmatrix}R^{(-)}R^{(+)}-T^{(-)}T^{(+)} & T^{(-)}\\ -T^{(+)} & 1\end{pmatrix} \tag{4}$$

A useful property of $\mathbf{N}$ is that its eigenvalues give the eigenvectors of $\mathbf{M}$ and vice-versa (McMahon 2018b). This simplifies expressions for wave transmission, reflection and energy exchanges in periodic structures. Applying Eqs.(4) and Eqs.(3a,b) to the two domains of the T-symmetric scattering model we find

$$\mathbf{M}=\frac{e^{i\left(\phi^{(+)}-\phi^{(-)}\right)/2}}{\sigma_0|T_0|}\begin{pmatrix}e^{i\bar{\phi}} & e^{-i\left(\chi^{(+)}-\chi^{(-)}\right)/2}e^{i\delta}\sigma_0^{(-)}|R_0|\\ -e^{i\left(\chi^{(+)}-\chi^{(-)}\right)/2}e^{i\delta}\sigma_0^{(+)}|R_0| & e^{-i\bar{\phi}}\end{pmatrix},\quad \mathbf{N}=\frac{e^{i\left(\chi^{(+)}-\chi^{(-)}\right)/2}e^{-i\delta}}{\sigma_0^{(-)}|R_0|}\begin{pmatrix}-e^{i\bar{\phi}} & e^{-i\left(\phi^{(+)}-\phi^{(-)}\right)/2}\sigma_0|T_0|\\ -e^{i\left(\phi^{(+)}-\phi^{(-)}\right)/2}\sigma_0|T_0| & e^{-i\bar{\phi}}\end{pmatrix} \tag{5}$$

The wave-scatterer energy exchange for the two domains of T-symmetry require evaluating the energy exchange matrix $\mathbf{X}=\mathbf{1}-\mathbf{S}^{*T}\mathbf{S}$ giving

$$\begin{aligned}\mathbf{X}&=-\left(\sigma_0^{(+)}-\sigma_0^{(-)}\right)|R_0|\begin{pmatrix}\sigma_0^{(+)}|R_0| & -e^{i\left(\phi^{(-)}-\phi^{(+)}\right)/2}\sigma_0|T_0|\\ -e^{-i\left(\phi^{(-)}-\phi^{(+)}\right)/2}\sigma_0|T_0| & -\sigma_0^{(-)}|R_0|\end{pmatrix},\ \sigma_0|T_0|\le 1,\ \delta=\pm\pi/2,\pm 3\pi/2\\ \mathbf{X}&=-\left(\sigma_0^{(+)}+\sigma_0^{(-)}\right)|R_0|\begin{pmatrix}\sigma_0^{(+)}|R_0| & -(\pm)ie^{i\left(\phi^{(-)}-\phi^{(+)}\right)/2}\sigma_0|T_0|\\ (\pm)ie^{-i\left(\phi^{(-)}-\phi^{(+)}\right)/2}\sigma_0|T_0| & \sigma_0^{(-)}|R_0|\end{pmatrix},\ \sigma_0|T_0|>1,\ \delta=0,\pm\pi\end{aligned} \tag{6}$$

The wave-scatterer energy exchanges are a sum of incoherent $F_{ex-incoh}$ (diagonal $\mathbf{X}$ terms) and coherent F_{ex-coh} (off-diagonal $\mathbf{X}$ terms):

$$\begin{aligned}F_{ex-incoh}&=-\sigma_0^{(+)}\left(\sigma_0^{(+)}-\sigma_0^{(-)}\right)|R_0|^2|A_n|^2+\sigma_0^{(-)}\left(\sigma_0^{(+)}-\sigma_0^{(-)}\right)|R_0|^2|B_{n+1}|^2,\ \sigma_0|T_0|\le 1\\ F_{ex-coh}&=2\sigma_0\left(\sigma_0^{(+)}-\sigma_0^{(-)}\right)|T_0||R_0|\cos\left(\alpha_n-\beta_{n+1}-\left(\phi^{(-)}-\phi^{(+)}\right)/2\right)|A_n||B_{n+1}|,\ \sigma_0|T_0|\le 1\\ F_{ex-incoh}&=-\sigma_0^{(+)}\left(\sigma_0^{(+)}+\sigma_0^{(-)}\right)|R_0|^2|A_n|^2-\sigma_0^{(-)}\left(\sigma_0^{(+)}+\sigma_0^{(-)}\right)|R_0|^2|B_{n+1}|^2,\ \sigma_0|T_0|>1\\ F_{ex-coh}&=(\pm)2\sigma_0\left(\sigma_0^{(+)}+\sigma_0^{(-)}\right)|T_0||R_0|\sin\left(\alpha_n-\beta_{n+1}-\left(\phi^{(-)}-\phi^{(+)}\right)/2\right)|A_n||B_{n+1}|,\ \sigma_0|T_0|>1\end{aligned} \tag{7}$$

where $A_n=|A_n|e^{i\alpha_n}$, $B_{n+1}=|B_{n+1}|e^{i\beta_{n+1}}$. F_{ex-coh} is phase dependent, requiring two simultaneous opposite travelling input waves, and involves interference of both reflections and forward transmissions (McMahon 2018b). Suppose $\sigma_0^{(+)}>\sigma_0^{(-)}$. From Eqs.(7) for $\sigma_0|T_0|\le 1$ *"A"* wave reflections contribute to a gain of incoherent wave energy while *"B"* wave reflections contribute an incoherent energy loss. For symmetric inelastic reflection

$\sigma_0^{(+)} = \sigma_0^{(-)}$ net incoherent energy exchanges are zero for $\sigma_0 |T_0| \le 1$ while nonzero and negative for $\sigma_0 |T_0| > 1$. In the latter case the scatterer is a source of energy stimulated by the input waves.

For nonreciprocal forward scattering where $\phi^{(-)}$ and $\phi^{(+)}$ are uncorrelated and random, ensemble averaging gives $\langle F_{ex-coh} \rangle = 0$ which is similar to the incoherent energy wave (IEW) model (McMahon 2015, 2016b). If the random phases preserve the difference $\delta = \bar{\chi} - \bar{\phi}$, it is similar to the non-BFW model (McMahon 2017a,b).

2.1 Wave scattering by cells of a periodic structure

A cell is defined as a nondispersive wave medium of length *d* in front of a "bare" scatterer of length *b*. The transfer matrix $\ddot{\mathbf{M}}$ for a cell introduces an explicit wavenumber dependence from propagation in the distance *d* whereas other parameters of "bare" scatterer $\mathbf{M}$ are implicitly wavenumber dependent. Wave propagation in a finite periodic structure of *m* identical cells is proportional to the *m*th power of $\ddot{\mathbf{M}}$. Wave propagation for any *m* is solved using the eigenvalues of $\ddot{\mathbf{M}}$ noting that powers of $\ddot{\mathbf{M}}$ have the same eigenvector (McMahon 2018a,b).

The derivation of $\ddot{\mathbf{M}}$ is almost identical to that of $\hat{\mathbf{M}}$ (McMahon 2018b) except both components of the wave vector $\begin{pmatrix} \ddot{A}_n & \ddot{B}_n \end{pmatrix}^T$ are at the entrance to the *n*th cell, and both components of the wave vector $\begin{pmatrix} \ddot{A}_{n+1} & \ddot{B}_{n+1} \end{pmatrix}^T$ are at the exit of the *n*th cell which is also the entrance to the *n*+1th cell. This gives for wavenumber k_s $\ddot{\mathbf{M}} = \mathbf{MU}$ which transforms Eqs.(1,4) by $T^{(\pm)} \to \ddot{T}^{(\pm)} = e^{ik_s d} T^{(\pm)}$, $R^{(-)} \to \ddot{R}^{(-)} = R^{(-)}$ and $R^{(+)} \to \ddot{R}^{(+)} = e^{2ik_s d} R^{(+)}$. The transformations are asymmetric in $e^{ik_s d}$ because the "bare" scatterer is located at the exit of the cell rather than in the middle. For brevity the following theory only treats cells but is easily applied to "bare" scatterers by $e^{\pm ik_s d} \to 1$. Solutions of the characteristic equations (CE) of $\ddot{\mathbf{M}}$ and $\ddot{\mathbf{N}}$ give the eigenvalues $\ddot{\gamma}^{(\pm)}$ and $\ddot{\rho}^{(\pm)}$, and eigenvectors $\begin{pmatrix} 1 & \ddot{\rho}^{(\pm)} \end{pmatrix}^T$ and $\begin{pmatrix} 1 & \ddot{\gamma}^{(\pm)} \end{pmatrix}^T$ as discussed in McMahon 2018b. This section writes $\ddot{\gamma}^{(\pm)}$ and $\ddot{\rho}^{(\pm)}$ in a form that clearly shows their relations to passing and stopping bands of an infinite periodic structure (McMahon 2015).

It is convenient to symmetrize $\ddot{\mathbf{M}}$ by defining $\tilde{\ddot{\mathbf{M}}} = \ddot{\mathbf{M}} / \sqrt{\det(\ddot{\mathbf{M}})}$, $\det(\ddot{\mathbf{M}}) = \ddot{T}^{(+)} / \ddot{T}^{(-)}$, $\det(\tilde{\ddot{\mathbf{M}}}) = 1$ with eigenvalues $\tilde{\ddot{\gamma}}^{(\pm)}$ and property $\tilde{\ddot{\gamma}}^{(-)} \tilde{\ddot{\gamma}}^{(+)} = 1$. Similarly $\tilde{\ddot{\mathbf{N}}} = \ddot{\mathbf{N}} / \sqrt{\det(\ddot{\mathbf{N}})}$, $\det(\ddot{\mathbf{N}}) = \ddot{R}^{(+)} / \ddot{R}^{(-)}$, $\det(\tilde{\ddot{\mathbf{N}}}) = 1$ with eigenvalues $\tilde{\ddot{\rho}}^{(\pm)}$, $\tilde{\ddot{\rho}}^{(-)} \tilde{\ddot{\rho}}^{(+)} = 1$. The diagonal matrix elements of $\tilde{\ddot{\mathbf{M}}}$ define $\tilde{\ddot{\Gamma}} = (\tilde{\ddot{M}}_{AA} + \tilde{\ddot{M}}_{BB})/2$ determining $\tilde{\ddot{\gamma}}^{(\pm)}$. Using the abreviation for any complex quantity $q = q' + iq''$ where q' denotes the real part and q'' denotes the imaginary part, the real and imaginary parts of $\tilde{\ddot{\gamma}}^{(\pm)}$ are

$$\tilde{\ddot{\gamma}}'^{(\pm)} = \tilde{\ddot{\Gamma}}' \left(1 - (\pm) \sqrt{\frac{\tilde{\ddot{\Delta}} - 1}{\tilde{\ddot{\Delta}} + 1}} \right), \quad \tilde{\ddot{\gamma}}''^{(\pm)} = \tilde{\ddot{\Gamma}}'' \left(1 - (\pm) \sqrt{\frac{\tilde{\ddot{\Delta}} + 1}{\tilde{\ddot{\Delta}} - 1}} \right), \quad \tilde{\ddot{\Delta}} = \left(\tilde{\ddot{\Gamma}}'^2 + \tilde{\ddot{\Gamma}}''^2 \right) + \sqrt{\left(1 - \left(\tilde{\ddot{\Gamma}}'^2 + \tilde{\ddot{\Gamma}}''^2 \right) \right)^2 + 4\tilde{\ddot{\Gamma}}''^2} \tag{8}$$

where $\tilde{\ddot{\Delta}}$ arises from the CE of the energy transfer matrix $\tilde{\ddot{\mathbf{E}}}$ with eigenvalues $\left| \tilde{\ddot{\gamma}}^{(\pm)} \right|^2$ (McMahon 2018b). For an infinite periodic structure unattenuated passing bands for elastic scattering correspond to $\tilde{\ddot{\Delta}} \to 1$ (taking the limit is needed to find the correct $\tilde{\ddot{\gamma}}''^{(\pm)}$) while stopping bands causing attenuation correspond to $\tilde{\ddot{\Delta}} > 1$ (McMahon 2015). The eigenvalues of $\tilde{\ddot{\mathbf{N}}}$ are given by

$$\tilde{\ddot{\rho}}'^{(\pm)} = \tilde{\ddot{\Omega}}' \left(1 - (\pm) \Upsilon_{\gamma\rho} \sqrt{\frac{\tilde{\ddot{\Phi}} - 1}{\tilde{\ddot{\Phi}} + 1}} \right), \quad \tilde{\ddot{\rho}}''^{(\pm)} = \tilde{\ddot{\Omega}}'' \left(1 - (\pm) \Upsilon_{\gamma\rho} \sqrt{\frac{\tilde{\ddot{\Phi}} + 1}{\tilde{\ddot{\Phi}} - 1}} \right), \quad \tilde{\ddot{\Phi}} = \left(\tilde{\ddot{\Omega}}'^2 + \tilde{\ddot{\Omega}}''^2 \right) + \sqrt{\left(1 - \left(\tilde{\ddot{\Omega}}'^2 + \tilde{\Omega}''^2 \right) \right)^2 + 4\tilde{\ddot{\Omega}}''^2} \tag{9}$$

where $\tilde{\ddot{\Omega}} = (\tilde{\ddot{N}}_{XX} + \tilde{\ddot{N}}_{YY})/2$, $\tilde{\ddot{\Phi}}$ arises in the CE of the energy reflection matrix $\tilde{\ddot{\mathbf{G}}}$ with eigenvalues $\left| \tilde{\ddot{\rho}}^{(\pm)} \right|^2$ (McMahon 2018b). For an infinite periodic structure passing bands correspond to $\tilde{\ddot{\Phi}} > 1$ while stopping bands

correspond to $\tilde{\tilde{\Phi}} \to 1$ (taking the limit is needed to find the correct $\tilde{\tilde{\rho}}''^{(\pm)}$) (McMahon 2018b). $\Upsilon_{\gamma\rho}$ is a factor that depends on the coupling of $\tilde{\tilde{\gamma}}^{(\pm)}$ with $\tilde{\tilde{\rho}}^{(\pm)}$ and has the value +1 or -1 but can change sign as a function of varying parameter values. These mutual constraints on $\ddot{\gamma}^{(\pm)}$ and $\ddot{\rho}^{(\pm)}$ are derived from generalizing Eqs.(1a) and (2a) of McMahon 2018b to cells. Introducing complex functions Υ_γ and Υ_ρ the general requirement is $\Upsilon_{\gamma\rho} = \Upsilon'_\gamma / \Upsilon'_\rho = \Upsilon''_\gamma / \Upsilon''_\rho = \pm 1$. This is satisfied for the two domains by

$$\Upsilon'_\gamma = \sigma_0 |T_0| \left(\cos(\bar{\phi}) \tilde{\tilde{\Gamma}}' \sqrt{\frac{\tilde{\tilde{\Delta}}-1}{\tilde{\tilde{\Delta}}+1}} - \sin(\bar{\phi}) \tilde{\tilde{\Gamma}}'' \sqrt{\frac{\tilde{\tilde{\Delta}}+1}{\tilde{\tilde{\Delta}}-1}} \right), \quad \Upsilon''_\gamma = \sigma_0 |T_0| \left(\sin(\bar{\phi}) \tilde{\tilde{\Gamma}}' \sqrt{\frac{\tilde{\tilde{\Delta}}-1}{\tilde{\tilde{\Delta}}+1}} + \cos(\bar{\phi}) \tilde{\tilde{\Gamma}}'' \sqrt{\frac{\tilde{\tilde{\Delta}}+1}{\tilde{\tilde{\Delta}}-1}} \right) \tag{10a}$$

$$\Upsilon'_\rho = \tilde{\sigma}_0 |R_0| \left(-\sin(\bar{\phi}) \tilde{\tilde{\Omega}}' \sqrt{\frac{\tilde{\tilde{\Phi}}-1}{\tilde{\tilde{\Phi}}+1}} - \cos(\bar{\phi}) \tilde{\tilde{\Omega}}'' \sqrt{\frac{\tilde{\tilde{\Phi}}+1}{\tilde{\tilde{\Phi}}-1}} \right), \quad \Upsilon''_\rho = \tilde{\sigma}_0 |R_0| \left(\cos(\bar{\phi}) \tilde{\tilde{\Omega}}' \sqrt{\frac{\tilde{\tilde{\Phi}}-1}{\tilde{\tilde{\Phi}}+1}} - \sin(\bar{\phi}) \tilde{\tilde{\Omega}}'' \sqrt{\frac{\tilde{\tilde{\Phi}}+1}{\tilde{\tilde{\Phi}}-1}} \right), \quad \sigma_0 |T_0| \le 1 \tag{10b}$$

$$\Upsilon'_\rho = \tilde{\sigma}_0 |R_0| \left(\cos(\bar{\phi}) \tilde{\tilde{\Omega}}' \sqrt{\frac{\tilde{\tilde{\Phi}}-1}{\tilde{\tilde{\Phi}}+1}} - \sin(\bar{\phi}) \tilde{\tilde{\Omega}}'' \sqrt{\frac{\tilde{\tilde{\Phi}}+1}{\tilde{\tilde{\Phi}}-1}} \right), \quad \Upsilon''_\rho = \tilde{\sigma}_0 |R_0| \left(\sin(\bar{\phi}) \tilde{\tilde{\Omega}}' \sqrt{\frac{\tilde{\tilde{\Phi}}-1}{\tilde{\tilde{\Phi}}+1}} + \cos(\bar{\phi}) \tilde{\tilde{\Omega}}'' \sqrt{\frac{\tilde{\tilde{\Phi}}+1}{\tilde{\tilde{\Phi}}-1}} \right), \quad \sigma_0 |T_0| > 1 \tag{10c}$$

2.2 Wave propagation in a finite periodic structure of *m* cells

Solving wave scattering by a finite periodic structure of *m* cells is equivalent to finding the forward transmission coefficients $\ddot{T}^{(\pm)(m)}$ and backward reflection coefficients $\ddot{R}^{(\pm)(m)}$ for use in matrices $\ddot{\mathbf{S}}^{(m)}$, $\ddot{\mathbf{M}}^{(m)}$ and $\ddot{\mathbf{N}}^{(m)}$. This can be done using the eigenvalues $\tilde{\tilde{\gamma}}^{(\pm)}$ and $\tilde{\tilde{\rho}}^{(\pm)}$ for a single cell (McMahon 2018a,b). Defining *m* cells as the start of the first "bare" scatterer to the end of the m^{th} "bare" scatterer then $\mathbf{M}^{(m)} = \ddot{\mathbf{M}}^m \mathbf{U}^{-1}$ which gives $T^{(\pm)(m)} = e^{-ik_s d} \ddot{T}^{(\pm)(m)}$, $R^{(+)(m)} = e^{-2ik_s d} \ddot{R}^{(+)(m)}$, $R^{(-)(m)} = \ddot{R}^{(-)(m)}$ that generalizes *m*=1 of subsect. 2.1. Applying the symmetrizing procedure of subsect. 2.1, the scattering coefficients for *m* cells are $\ddot{T}^{(+)(m)} = \det(\ddot{\mathbf{M}})^{m/2} \tilde{\tilde{T}}^{(m)}$, $\ddot{T}^{(-)(m)} = \det(\ddot{\mathbf{M}})^{-m/2} \tilde{\tilde{T}}^{(m)}$, $\ddot{R}^{(+)(m)} = \det(\ddot{\mathbf{N}})^{1/2} \tilde{\tilde{R}}^{(m)}$, $\ddot{R}^{(-)(m)} = \det(\ddot{\mathbf{N}})^{-1/2} \tilde{\tilde{R}}^{(m)}$. Note properties $\tilde{\tilde{T}}^{(m)} = \sqrt{\ddot{T}^{(-)(m)} \ddot{T}^{(+)(m)}}$ and $\tilde{\tilde{R}}^{(m)} = \sqrt{\ddot{R}^{(-)(m)} \ddot{R}^{(+)(m)}}$. The symmetrized transmission and reflection coefficients for *m* cells, in terms of single cell eigenvalues, can be derived from the eigenvalue/eigenvector equations for $\tilde{\tilde{\mathbf{M}}}^m$ noting that its eigenvectors $\begin{pmatrix} 1 & \tilde{\tilde{\rho}}^{(\pm)} \end{pmatrix}^T$ do not depend on *m*. This gives

$$\tilde{\tilde{T}}^{(m)} = \frac{\tilde{\tilde{\rho}}^{(-)} - \tilde{\tilde{\rho}}^{(+)}}{\tilde{\tilde{\gamma}}^{(-)m} \tilde{\tilde{\rho}}^{(-)} - \tilde{\tilde{\gamma}}^{(+)m} \tilde{\tilde{\rho}}^{(+)}}, \quad \tilde{\tilde{R}}^{(m)} = \frac{\tilde{\tilde{\gamma}}^{(-)m} - \tilde{\tilde{\gamma}}^{(+)m}}{\tilde{\tilde{\gamma}}^{(-)m} \tilde{\tilde{\rho}}^{(-)} - \tilde{\tilde{\gamma}}^{(+)m} \tilde{\tilde{\rho}}^{(+)}} \tag{11}$$

There is no *m* dependence for $\tilde{\tilde{\rho}}^{(\pm)}$ terms because $\ddot{\mathbf{N}}^{(m)}$ is not simply proportional to the m^{th} power of $\ddot{\mathbf{N}}$. Introducing the phases $\tilde{\tilde{\varphi}}'$ and $\tilde{\tilde{\vartheta}}'$ where $\tilde{\tilde{\gamma}}^{(\pm)} = \left|\tilde{\tilde{\gamma}}^{(\pm)}\right| e^{\pm i\tilde{\tilde{\varphi}}'}$ and $\tilde{\tilde{\rho}}^{(\pm)} = \left|\tilde{\tilde{\rho}}^{(\pm)}\right| e^{\pm i\tilde{\tilde{\vartheta}}'}$ Eqs.(11) leads to

$$\left|\tilde{\tilde{T}}^{(m)}\right|^2 = \frac{\left|\tilde{\tilde{\rho}}^{(\pm)}\right|^{-2} + \left|\tilde{\tilde{\rho}}^{(\pm)}\right|^2 - 2\cos(2\tilde{\tilde{\vartheta}}')}{\left|\tilde{\tilde{\gamma}}^{(\pm)}\right|^{-2m} \left|\tilde{\tilde{\rho}}^{(\pm)}\right|^{-2} + \left|\tilde{\tilde{\gamma}}^{(\pm)}\right|^{2m} \left|\tilde{\tilde{\rho}}^{(\pm)}\right|^2 - 2\cos(2m\tilde{\tilde{\varphi}}' + 2\tilde{\tilde{\vartheta}}')}, \quad \left|\tilde{\tilde{R}}^{(m)}\right|^2 = \frac{\left|\tilde{\tilde{\gamma}}^{(\pm)}\right|^{-2m} + \left|\tilde{\tilde{\gamma}}^{(\pm)}\right|^{2m} - 2\cos(2m\tilde{\tilde{\varphi}}')}{\left|\tilde{\tilde{\gamma}}^{(\pm)}\right|^{-2m} \left|\tilde{\tilde{\rho}}^{(\pm)}\right|^{-2} + \left|\tilde{\tilde{\gamma}}^{(\pm)}\right|^{2m} \left|\tilde{\tilde{\rho}}^{(\pm)}\right|^2 - 2\cos(2m\tilde{\tilde{\varphi}}' + 2\tilde{\tilde{\vartheta}}')} \tag{12}$$

where $(\pm)$ equivalence applies since $\left|\tilde{\tilde{\gamma}}^{(+)}\right|\left|\tilde{\tilde{\gamma}}^{(-)}\right| = 1$, $\left|\tilde{\tilde{\rho}}^{(+)}\right|\left|\tilde{\tilde{\rho}}^{(-)}\right| = 1$.

$\tilde{\tilde{\mathbf{M}}}^2$ is easily evaluated for *m*=2 by direct multiplication and gives the analytical results

$$\left|\tilde{\tilde{T}}^{(2)}\right|^2 = \frac{{\sigma_0}^4 |T_0|^4}{{\sigma_0}^4 |T_0|^4 + 4\left(1 - {\sigma_0}^2 |T_0|^2\right)\cos^2(\zeta)}, \quad \left|\tilde{\tilde{R}}^{(2)}\right|^2 = \frac{4{\tilde{\sigma}_0}^2 |R_0|^2 \cos^2(\zeta)}{{\sigma_0}^4 |T_0|^4 + 4\left(1 - {\sigma_0}^2 |T_0|^2\right)\cos^2(\zeta)} \tag{13}$$

where $\zeta = k_s d + \bar{\phi}$. Direction dependence is given by $\left|T^{(\pm)(2)}\right|^2 = \left|\tilde{\bar{T}}^{(2)}\right|^2$ and $\left|R^{(\pm)(2)}\right|^2 = \left|\tilde{\bar{R}}^{(2)}\right|^2 \sigma_0^{(\pm)} / \sigma_0^{(\mp)}$. At the EP $\sigma_0 |T_0| = 1$, $\sigma_0^{(+)}\sigma_0^{(-)} = 0$ and suppose $\sigma_0^{(+)} = 0$, $\sigma_0^{(-)} \neq 0$. $\left|R^{(+)(2)}\right|^2 = 0$ while $\left|R^{(-)(2)}\right|^2 > 0$ hence is unidirectional invisibility. Transmission is unattenuated in both directions. Despite $\sigma_0^{(-)} \neq 0$ *"B"* wave transmission is unattenuated because the scatterer injects extra energy. This is seen from wave-scatterer energy exchanges for unit incident flux $F_{ex-incoh}^{(\pm)(2)} = 1 - \left|T^{(\pm)(2)}\right|^2 - \left|R^{(\pm)(2)}\right|^2$ giving $F_{ex-incoh}^{(+)(2)} = 0$ and $F_{ex-incoh}^{(-)(2)} < 0$. In general PT-symmetric scatterers at the EP are energy sources for one of the incident flux directions, hence are active systems. The domain $\sigma_0 |T_0| > 1$ is always a wave energy source and as seen from Eqs.(13), and since damping is not included, gives divergent energy emissions for $\sigma_0 |T_0| = \sqrt{2}$ and $k_s d + \bar{\phi} = n\pi$, n=0, ±1, ±2.. coinciding with the wavelengths of Bragg reflections. These emissions include reflections that are asymmetric for $\sigma_0^{(+)} \neq \sigma_0^{(-)}$ and can be different to emissions in the same direction as the incident flux. Such large wave amplifications are limited by the energy supply to PT-symmetric scatterers. Analysis of the denominator of Eqs.(12) shows the divergence condition is $\sigma_0 |T_0| = \sqrt{2}$ for all m=2n where n is an odd integer.

3 NUMERICAL EXAMPLES OF PT SYMMETRY AND BROKEN PT SYMMETRY WAVE EFFECTS

Reciprocity $\phi^{(+)} = \phi^{(-)} = \bar{\phi}$ is assumed for all figures. Figures 1 and 2 demonstrate the features of PT-symmetry versus $\sigma_0 |T_0|$ for $k_s d / \pi = 0$ approximating wavelengths much larger than spacing d. For Figs.1 & 2 $\bar{\phi} / \pi = 0.2564$, $\cos(\bar{\phi}) = 0.6927$, $\sigma_0 = 1.95$, $\sigma_0^{(-)} = 1$, for $\sigma_0 |T_0| \leq 1$, $\bar{\chi} / \pi = 0.7564$, $\bar{\delta} / \pi$=0.5 and for $\sigma_0 |T_0| > 1$, $\bar{\chi} / \pi = 0.2564$, $\bar{\delta} / \pi$=0. Parameters σ_0 & $\sigma_0^{(-)}$ are constant so that $\sigma_0^{(+)}$ & $|R_0|$ depend on $\sigma_0 |T_0|$ to conform to Eqs.(3a,b). The real and imaginary parts of the eigenvalues $\tilde{\bar{\gamma}}^{(\pm)}$ and $\tilde{\bar{\rho}}^{(\pm)}$ versus $\sigma_0 |T_0|$ are plotted in Fig. 1. It shows that $\tilde{\bar{\gamma}}^{(\pm)}$ is real for the stopping band and complex for the passing band, contrasting with $\tilde{\bar{\rho}}^{(\pm)}$ which is complex for the stopping band and real for the passing band, but only for PT-symmetry $\sigma_0 |T_0| < 1$. For broken symmetry $\sigma_0 |T_0| > 1$, which is a passing band, $\tilde{\bar{\rho}}^{(\pm)}$ is imaginary. At the EP $\sigma_0 |T_0| = 1$ $\tilde{\bar{\rho}}^{(\pm)}$ are zeros and negative infinities in the real and imaginary parts while $\tilde{\bar{\gamma}}^{(\pm)}$ are continuous.

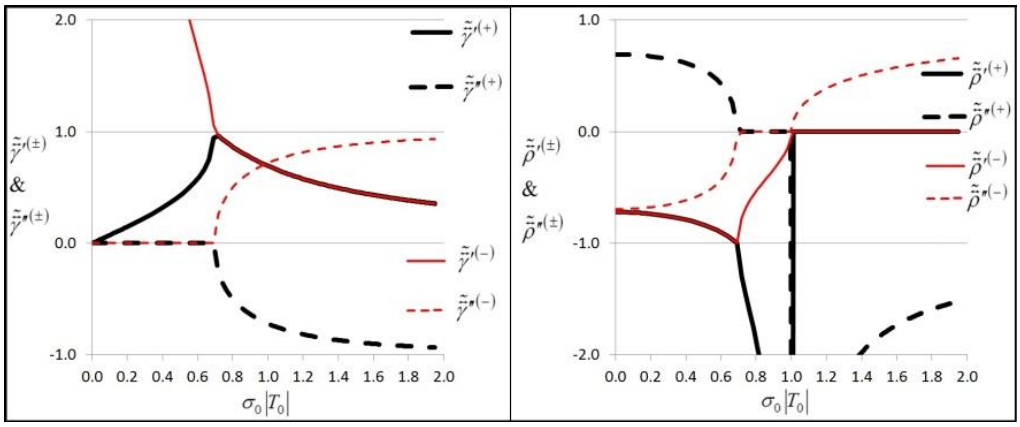

Figure 1: Real and imaginary parts of the eigenvalues $\tilde{\bar{\gamma}}^{(\pm)}$ and $\tilde{\bar{\rho}}^{(\pm)}$.

Figure 2 compares symmetrized energy transmission $\left|\tilde{\bar{T}}^{(m)}\right|^2$ and reflection $\left|\tilde{\bar{R}}^{(m)}\right|^2$ coefficients for different size structures m=3 and 6. Maxima and minima are from scattered coherent wave interference. A general property

demonstrated is $\left|\tilde{\tilde{T}}^{(m)}\right|^2+\left|\tilde{\tilde{R}}^{(m)}\right|^2=1$ for PT-symmetry $\sigma_0|T_0|\le 1$ and $\left|\tilde{\tilde{T}}^{(m)}\right|^2+\left|\tilde{\tilde{R}}^{(m)}\right|^2>1$ for broken symmetry $\sigma_0|T_0|>1$. For all *m* there is a zero in $\left|\tilde{\tilde{R}}^{(m)}\right|^2$ at the EP $\sigma_0|T_0|=1$ caused by the $\sigma_0^{(+)}=0$ giving unidirectional "invisibility". The other deep minima in $\left|\tilde{\tilde{R}}^{(m)}\right|^2$ are also zeros. Analysis of Eqs. (12) shows that these reflection coefficient zeros only occur in a passing band which is $\sigma_0|T_0|>0.6927$ in these examples. Since $\sigma_0|T_0|\neq 1$ and $\sigma_0^{(\pm)}\neq 0$ these zeros can only arise from multiple scattering between scatterers and give bidirectional "invisibility". Equation (12) shows that the reflectivity zeros are at $\left(\sigma_0|T_0|\right)_{m,n}=\cos(\bar{\phi})/\cos(n\pi/m)$, n=1,.2,.., which is confirmed numerically in Fig. 2 for *m*=3 and 6 where $\left(\sigma_0|T_0|\right)_{3,1}=1.3854$ and $\left(\sigma_0|T_0|\right)_{6,1}=0.8$, $\left(\sigma_0|T_0|\right)_{6,2}=1.3854$.

Figures 3, 4 and 5 demonstrate the wavenumber dependence of PT and broken PT symmetry. In all cases $\bar{\phi}/\pi=0.2564$, $\sigma_0^{(-)}=1$ and $\sigma_0=1.95$. For PT-symmetry $\sigma_0|T_0|=0.85$, $|R_0|=0.9$, $\bar{\chi}/\pi=0.7564$, $\bar{\delta}/\pi$=0.5, $\sigma_0^{(+)}=0.3426$. Broken PT symmetry uses $\sigma_0|T_0|=\sqrt{2}$, $|R_0|=0.96885$, $\bar{\chi}/\pi=0.2564$, $\bar{\delta}/\pi$=0, $\sigma_0^{(+)}=2.1095$. Passing and stopping bands are clearly distinguished in Fig. 3 that plots the real and imaginary parts of $\tilde{\tilde{\gamma}}^{(\pm)}$. For passing bands $\left|\tilde{\tilde{\gamma}}'^{(\pm)}\right|\le 1$, $\left|\tilde{\tilde{\gamma}}''^{(\pm)}\right|\le 1$ whereas stopping bands only occur for PT symmetry and have eigenvalues

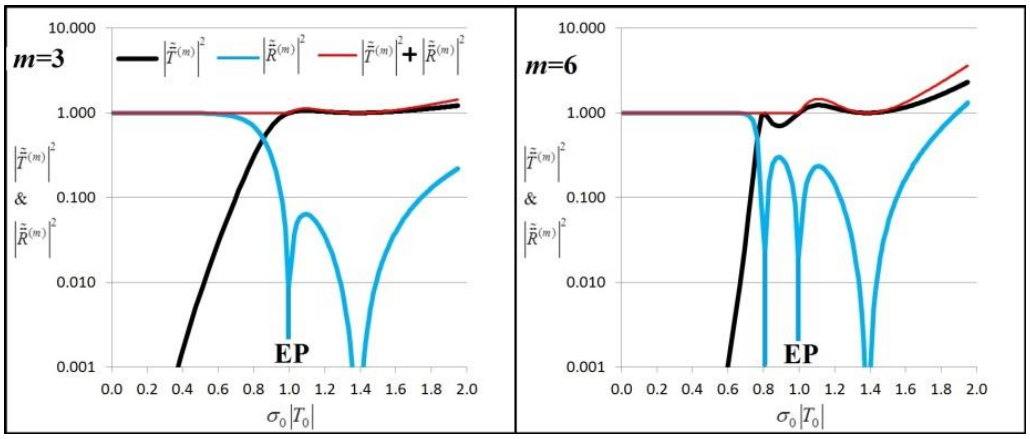

Figure 2: PT-symmetry and broken symmetry transmission and reflection coefficients for *m*=3 and 6. For all *m* unidirectional invisibility for all *m* occurs at the EP due to $\sigma_0^{(+)}=0$. Bidirectional invisibility are reflection zeros at wavenumbers that depend on m.

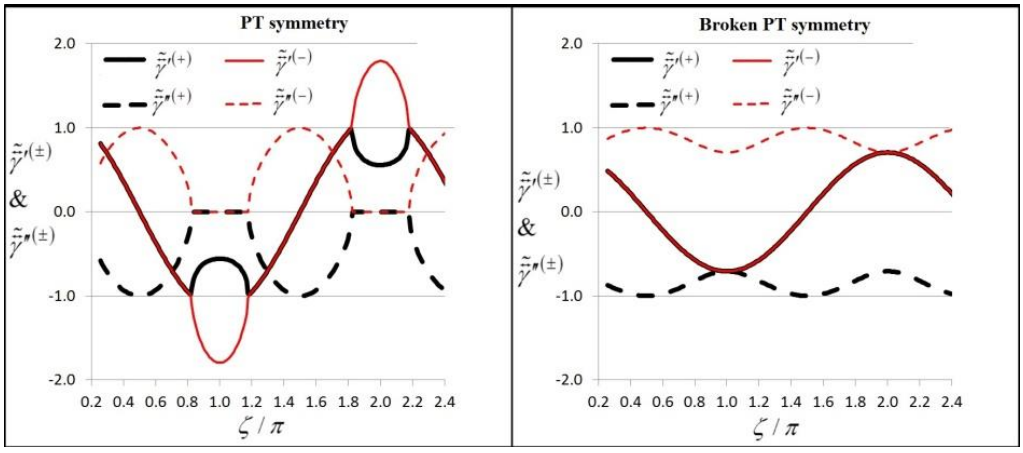

Figure 3: Symmetrized real and imaginary parts of the eigenvalues $\tilde{\tilde{\gamma}}^{(\pm)}$ of $\tilde{\tilde{\mathbf{M}}}$ versus ζ/π.

$\left|\tilde{\tilde{\gamma}}'^{(-)}\right|>1,\ \tilde{\tilde{\gamma}}''^{(\pm)}=0$. Stopping bands for PT symmetry are centred on the Bragg reflection wavenumbers at $\zeta_n/\pi=n$, n=1,2,... Eigenvalues $\tilde{\tilde{\rho}}^{(\pm)}$ (not shown) are $\left|\tilde{\tilde{\rho}}'^{(+)}\right|>1$ or $\left|\tilde{\tilde{\rho}}'^{(-)}\right|>1,\ \tilde{\tilde{\rho}}''^{(\pm)}=0$ for PT symmetry passing bands and $\left|\tilde{\tilde{\rho}}'^{(\pm)}\right|<1,\ \left|\tilde{\tilde{\rho}}''^{(\pm)}\right|<1$ for stopping bands, and $\tilde{\tilde{\rho}}'^{(\pm)}=0$ for broken symmetry passing band. Broken PT symmetry in Fig. 3 shows equal real and imaginary parts of $\tilde{\tilde{\gamma}}^{(\pm)}$ at $\zeta_n/\pi=n$, n=1,2,.. Bragg reflection wavenumbers. This only occurs for $\sigma_0|T_0|=\sqrt{2}$ and gives rise to divergent scattering coefficients discussed in Subsect. 2.2.

Figure 4 compares the broken PT symmetry transmission and reflection coefficients for m=3 and 6. This also shows that $\left|\tilde{\tilde{T}}^{(m)}\right|^2-\left|\tilde{\tilde{R}}^{(m)}\right|^2=1$ generalizing single scatterer properties Eqs.(3a,b). Forward scattering is mostly amplified $\left|\tilde{\tilde{T}}^{(m)}\right|^2>1$ whereas reflection is mostly attenuated $\left|\tilde{\tilde{R}}^{(m)}\right|^2<1$. The large amplification of transmission and reflection for m=6 but not m=3 at the Bragg wavenumbers exemplifies the divergent gain condition $\sigma_0|T_0|=\sqrt{2}$, m=2n for n an odd integer.

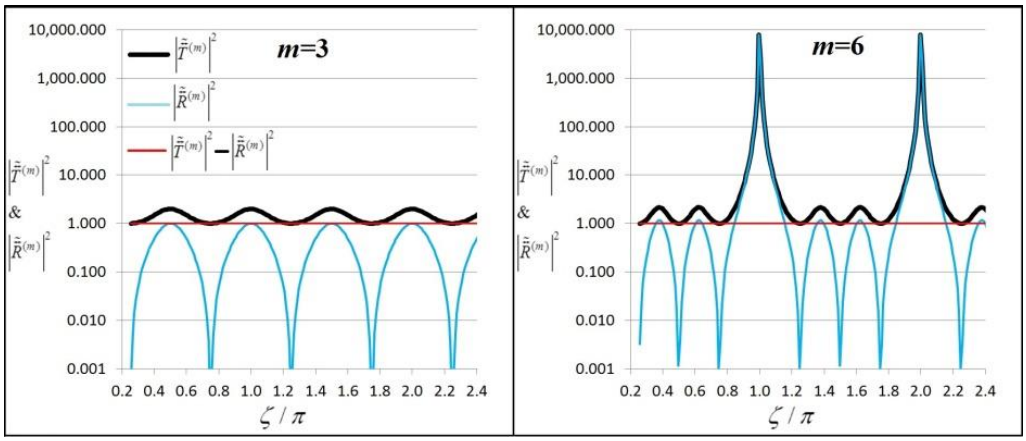

Figure 4. Symmetrized transmission and reflection versus ζ/π for m=3 and 6 broken PT symmetry.

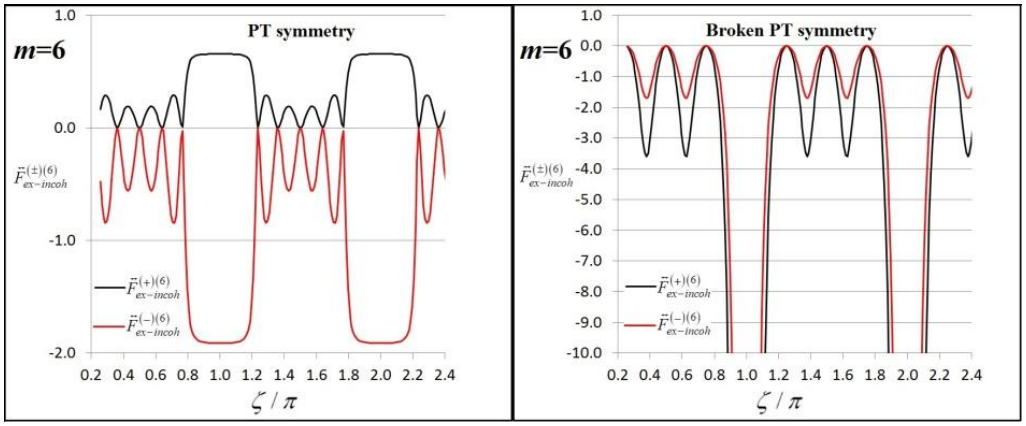

Figure 5: Wave – periodic structure energy exchanges versus ζ/π for m=6 PT and broken PT symmetry.

Figure 5 compares wave-scatterer energy exchanges for A-wave and B-wave incident onto a m=6 finite periodic structure. For PT symmetry there is net energy absorption of the A-wave, and net amplification for the B-wave, in the stopping bands centred around the Bragg reflection wavenumbers. All of the broken symmetry domain,

nulls at except discrete wavenumbers, gives amplification for both incident wave directions. As discussed previously the broken symmetry amplification diverges at the Bragg wavenumbers.

4 FINAL REMARKS

PT symmetry and broken PT symmetry for waves in periodic structures has two main surprises. One is bidirectional invisibility in passing bands which requires a minimum of 3 scatterers. The other is very large amplification of waves at the Bragg wavelengths in the broken PT domain for a minimum of 2 scatterers. It is worth investigating if the reverse case of very large damping of waves could happen with other scattering models. So far there has been no experimentation to test these predicted PT symmetry properties of periodic structures.

REFERENCES

Auregan, Y. and Pagneux, V. 2017. 'PT-Symmetric Scattering in Flow Duct Acoustics', *Phys. Rev. Lett.* **118**, 174301.

Bender, C. 2007. 'Making Sense of Non-Hermitian Hamiltonians*', Rep. Prog. Phys.* **70**, 947.

Brillouin, L. 1953. *Wave Propagation in Periodic Structures*, Second Edition, Dover Publications, INC.

El-Ganainy, R., Makris, K. G., Khajavikhan, M., Musslimani, Z. H., Rotter, S. and Christodoulides, D. N. 2018, 'Non-Hermitian physics and PT symmetry', *Nature Physics*, **14** January, www.nature.com/naturephysics.

Feng, L., Xu, Y. L., Fegadolli, W.S., Lu, M.H., Oliveira, J. E., Almeida, V.R., Chen, Y-F. and Scherer, A. 2013. 'Experimental demonstration of a unidirectional reflectionless parity-time metamaterial at optical frequencies', *Nat. Mater.* **12** 108–13.

Fleury, R., Sounas, D. L., Haberman, M. R., Alù, A., 2015. 'Nonreciprocal Acoustics', *Acoustics Today*, 11 (3), 14 – 21.

Ge, L., Chong Y.D. and Stone, A. D. 2012. 'Conservation relations and anisotropic transmission resonances in one-dimensional PT-symmetric photonic heterostructures', DOI: 10.1103/PhysRevA.85.023802.

Gu, Z., Jie Hu, J., Bin Liang, B., Zou, X., and Cheng, J. 2016. 'Broadband non-reciprocal transmission of sound with invariant frequency', *Sci. Rep.* **6**, 19824; doi: 10.1038/srep19824.

Lin, Z., Ramezani, H., Eichelkraut, T., Kottos, T., Cao, H. and Christodoulides, D. N. 2011. 'Unidirectional invisibility induced by PT-symmetric periodic structures', *Phys. Rev. Lett.* **106**, 213901.

Longhi, S. 2011. 'Invisibility in PT-symmetric complex crystals', *J. Phys. A* **44**, 485302.

Maznev, A.A., Every, A.G. and Wright, O.B. 2013. 'Reciprocity in reflection and transmission: What is a 'phonon diode'?', *Wave Motion* 50, 776–784.

McMahon, D. 2015. 'Wave propagation in infinite periodic structures taking into account energy absorption', *Proceedings of Acoustics 2015*, Hunter Valley, Australia.

McMahon, D. 2016a. 'Wave propagation in infinite periodic structures', *Proceedings of the 23rd International Congress on Sound and Vibration (ICSV23)*, Athens, Greece.

McMahon, D. 2016b. 'Symmetry of waves in an infinite 1D periodic structure under the interchange of forward and backward scattering coefficients', *Proceedings of Acoustics 2016*, Brisbane, Australia.

McMahon, D. 2017a. 'Wave propagation and attenuation in an infinite periodic structure of asymmetric scatterers', *Proceedings of the 24th International Congress on Sound and Vibration (ICSV24)*, London, UK.

McMahon, D. 2017b. 'Relative performance of different strategies for wave attenuation by periodic structures', *Proceedings of Acoustics 2017*, Perth, Australia.

McMahon, D. 2018a. 'Coherent and incoherent waves within a one dimensional periodic structure of point scatterers including boundaries', *Proceedings of the 25th International Congress on Sound and Vibration (ICSV25)*, Hiroshima, Japan.

McMahon, D. 2018b. 'Coherent waves in finite, asymmetric, one dimensional periodic structures', *Proceedings of Acoustics 2018*, Adelaide, Australia.

Mostafazadeh, A. 2013. 'Invisibility and PT symmetry', *Phys. Rev. A* 87, 012103.

Pierce, A. D. 1981. *Acoustics: An Introduction to Its Physical Principles and Applications,* Acoustical Society of America, Woodbury, NY.

Regensburger A., Bersch C., Miri M-A., Onishchukov G., Christodoulides D. N. and Peschel, U. 2012. 'Parity-time synthetic photonic lattices', *Nature* 488 167–71.

Shi C., Dubois M., Chen Y., Cheng L., Ramezani H., Wang Y. and Zhang X. 2016. 'Accessing the exceptional points of parity-time symmetric acoustics', *Nat. Commun.* 7:11110 doi: 10.1038/ncomms11110.

Schomerus, H. 2013. 'From scattering theory to complex wave dynamics in non-Hermitian *PT*-symmetric resonators', *Phil Trans R Soc A* 371: 20120194. http://dx.doi.org/10.1098/rsta.2012.0194.

Sounas, D.L., Fleury, R. and Alù, A. 2015. 'Unidirectional cloaking based on metasurfaces with balanced loss and gain', *Phys. Rev. Appl.* **4** 014005.